Modeling of Wheeled Inverted Pendulum Systems

Ulrike Zwiers
Faculty of Mechatronics and Mechanical Engineering
Bochum University of Applied Sciences, Germany
Email: ulrike.zwiers@hs-bochum.de

***Abstract*—In this paper, the modeling of wheeled inverted pendulum systems is revisited. Such mobile robots are widely used in research and education to explore and exemplify the control of inherently unstable, under-actuated systems. But despite of the numerous studies in this field, many authors apparently fail to derive the model equations adequately as shown by means of the dynamical model of a planar wheel-rod system. Focussing on the correct handling of the driving torque, the model is developed using both Newtonian and Lagrangian mechanics approaches. Finally, the resulting nonlinear model is compared against a model commonly found in literature by numerical simulation.**

This paper does not only highlight a widespread misconception in modeling mechanical systems, namely the difference between applied and reaction forces and torques, respectively, but suggests a demonstrative way of teaching this particular issue in both undergraduate and graduate courses on engineering mechanics.

***Keywords*—Mobile robot, wheeled inverted pendulum, Lagrangian/ Newtonian mechanics, generalized forces**

I. Introduction

The study documented in this paper is inspired by the well-known self-balancing *Segway*® robot [1] which has attracted intense research interest in recent years. Basically, the *Segway*® robot is similar to the classical control problem of an inverted pendulum on a cart [2], even though wheeled locomotion includes additional challenges like wheel slip, non-holonomy (in case of spatial motion), and multiple control input (in case of the popular two-wheeled robot, for example). But while inverted pendulums rarely occur in useful products due to their unstable dynamics, the *Segway*® robot as a commercial implementation of a two-wheeled inverted pendulum actually represents a serious contribution to personal human transportation. However, featuring high maneuverability and small footprint, various designs of two-wheeled inverted pendulum systems are documented in literature.

The *Yamabico Kurara* robot developed by Ha and Yuta [3] in 1996 may be considered as the first prototype of a wheeled inverted pendulum vehicle actuated by two independent driving wheels on the same axle and equipped with a gyro type sensor to measure the inclination angle and angular velocity of the pendulum body. *JOE* is another implementation of a two-wheeled robot stabilized by a linear state space controller and scaled down with a constant weight attached to the pendulum body to simulate a human driver [4]. Besides those mobile research platforms used for diverse scientific studies within the field of control theory and robotics, the development of low-cost wheeled inverted pendulum systems is documented, e. g. based on *LEGO Mindstorms*® [5], which are mainly designed for educational purpose.

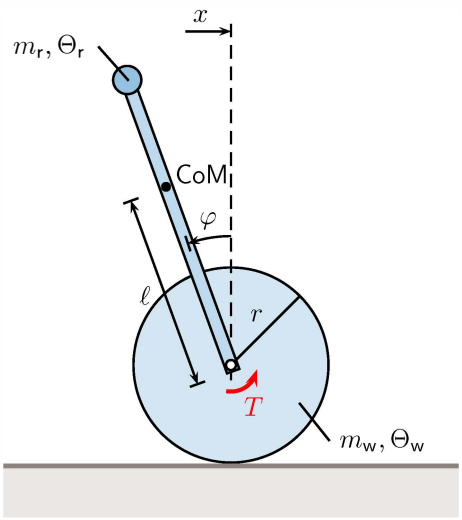

Fig. 1. Planar wheeled inverted pendulum

But regardless of the actual purpose of development, most mobile inverted pendulums use model-based controllers, that is, their control utilizes a mathematical model of the system. A review of the relevant literature, however, reveals an frequently incorrect modeling of the motor torque(s) driving the vehicles. This issue is elaborated in the sequel, referring to the planar wheeled inverted pendulum sketched in Figure 1.

A. System Description

The system under consideration consists of a rigid rod pivot-mounted on the axle of a wheel which is actuated by a torque that drives the system along a horizontal track (Fig. 1). The revolute joint connecting the rod and the wheel is modeled as an ideal one, that is, without friction or clearance. Assuming slip-free rolling of the wheel, the system features two degrees of freedom, which correspond to the horizontal position of the wheel, x, and the inclination angle of the rod with respect to the vertical axis, φ. Obviously, $\varphi = 0$ represents the unstable equilibrium of the system. As there

TABLE I
LIST OF MODEL PARAMETERS

Symbol	Value	Unit	Description
m_r	2	kg	Mass of the rod
Θ_r	0.15	$\mathsf{kg\,m^2}$	Mass moment of inertia of the rod
m_w	5	kg	Mass of the wheel
Θ_w	0.04	$\mathsf{kg\,m^2}$	Mass moment of inertia of the wheel
ℓ	400	mm	Distance between the center of mass (CoM) of the rod and its pivoted end
r	100	mm	Radius of the wheel
g	9.81	$\mathsf{m\,s^{-2}}$	Gravitational acceleration
T		Nm	Driving torque

is only one control input, namely the driving torque, the system is to be classified as under-actuated. The parameters of the model, their descriptions and their values[1] used in the numerical simulations documented in Section III are listed in Table I.

Referring to a right-handed coordinate system with a positive angle producing a counter-clockwise rotation as viewed from the positive end of the axis looking toward the origin, the position of the rod's center of mass is given by

$$\boldsymbol{r}_\mathsf{r} = \begin{bmatrix} x - \ell \sin\varphi \\ \ell \cos\varphi \end{bmatrix} . \tag{1}$$

As the wheel is supposed to roll without sliding, the rotation of the wheel can be expressed in terms of its horizontal displacement. Thus, the translational velocity of the wheel's center, $\dot{x}$, and its angular velocity $\dot{\psi}$ are linked by the constraint equation

$$\dot{x} = -\dot{\psi} r . \tag{2}$$

Integrating (2) yields the horizontal position of the wheel,

$$x = x_0 - \psi r , \tag{3}$$

with x_0 and ψ denoting the initial position and the rotation angle of the wheel, respectively.

B. Benchmark Model

Using a harmonized notation, the models of wheeled inverted pendulum systems frequently documented in both project theses and scientific papers, for example, in [4], [6], [7], [8], [9], [10], are now narrowed down to a common benchmark model allegedly representing the planar wheel-rod system described above. That is, even though most models described in literature cover spatial motion and incorporate additional effects, such as friction in the bearings, slippage of the wheel(s) and characteristics of the motor(s), the modeling of a severely simplified system is addressed in order to focus on a particular issue that turned out to be critical, namely the correct handling of the motor torque(s)[2].

Thus, the two-degrees-of-freedom benchmark model is supposed to be of the form

$$\boldsymbol{M}(\varphi) \begin{bmatrix} \ddot{\varphi} \\ \ddot{x} \end{bmatrix} = \boldsymbol{f}(\varphi, \dot{\varphi}) - \begin{bmatrix} 1 \\ 1 \end{bmatrix} T , \tag{4}$$

with the mass matrix $\boldsymbol{M}$ and the vector function $\boldsymbol{f}$ being specified in Section III. Obviously, the motor torque T appears in both differential equations, which conflicts with expectation as the motor torque is an applied torque solely driving the wheel. In the papers cited above, however, the motor torque is treated as a reaction torque acting on both the wheel and the rod.

II. MODELING

For mechanical systems, the two most common formalisms to derive the governing dynamic equations are known as Newtonian mechanics and Lagrangian mechanics. The main difference between the two approaches concerns the handling of constraints. While in Newtonian mechanics, each body is treated separately and the constraints are modeled explicitly through the forces required to enforce them, the Lagrangian approach provides a systematic, energy-based procedure for eliminating the constraints from the dynamic model. Even though both approaches leads to equivalent equations, their mathematical description differs with respect to their ability to give insights into the underlying mechanical problem, which motivates the modeling of the wheeled inverted pendulum using both the Newtonian and the Lagrangian approach, as documented in the sequel.

A. Newtonian Approach

As customary in Newtonian mechanics, a free-body diagram of the system of interest is drawn first. Referring to the one shown in Figure 2, F_N and F_T denote the normal and tangential components of the contact force, with F_T being the static friction force that allows for ideal rolling, and F_x and F_y are the reaction forces associated with the revolute joint. Such a joint cannot transmit torques, that is, the driving torque T acts only on the wheel.

The equations of motion of the wheel read as

$$\begin{aligned} m_\mathsf{w}\ddot{x} &= F_\mathsf{T} + F_x , \\ 0 &= F_\mathsf{N} - F_y - m_\mathsf{w} g , \\ \Theta_\mathsf{w}\ddot{\psi} &= F_\mathsf{T} r + T , \end{aligned} \tag{5}$$

[1] The provided values are approximated for an experimental setup of a wheeled inverted pendulum planned to be built.

[2] Another common mistake found in literature concerns the sign in the rolling constraint (2). Some authors take the absolute values of the velocities, which results in an inconsistent modeling regarding the signs of the angular quantities, i. e., the inclination angle of the rod, φ, and the rotation angle of the wheel, ψ. But since this discrepancy can easily be overcome by strictly applying the right-hand rule, the benchmark model is assumed to feature correct signs as introduced previously.

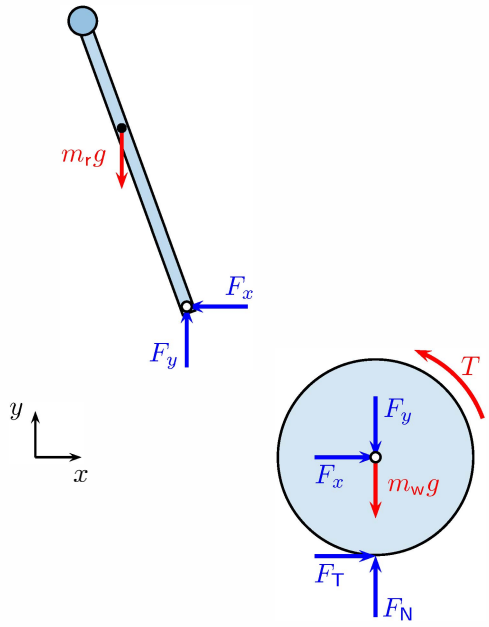

Fig. 2. Free-body diagram

while the dynamic equilibrium of the rod is governed by the balance equations

$$\begin{aligned} m_\mathrm{r}\ddot{x}_\mathrm{r} &= -F_x \,, \\ m_\mathrm{r}\ddot{y}_\mathrm{r} &= F_y - m_\mathrm{r} g \,, \\ \Theta_\mathrm{r}\ddot{\varphi} &= -F_x \ell\cos\varphi + F_y \ell \sin\varphi \,. \end{aligned} \tag{6}$$

Substituting $(6)_1$ and $(6)_2$ into $(6)_3$ and replacing $\ddot{x}_\mathrm{r}$ and $\ddot{y}_\mathrm{r}$ by the second time derivative of (1) yields

$$\Theta_\mathrm{r}\ddot{\varphi} = m_\mathrm{r}\ell\ddot{x}\cos\varphi - m_\mathrm{r}\ell^2\ddot{\varphi} + m_\mathrm{r} g\ell\sin\varphi \,. \tag{7}$$

In an analogous manner, the substitution of $(5)_1$ and $(6)_1$ into $(5)_3$ and using the time derivatives of (1) and (2) leads to

$$\frac{\Theta_\mathrm{w}}{r}\ddot{x} = m_\mathrm{r} r\ell(\ddot{\varphi}\cos\varphi - \dot{\varphi}^2\sin\varphi) - (m_\mathrm{w} + m_\mathrm{r})r\ddot{x} - T. \tag{8}$$

B. Lagrangian Approach

For mechanical systems with n degrees of freedom featuring only holonomic constraints, the Lagrange equation can be expressed in terms of the n generalized coordinates q_i as

$$\frac{\mathrm{d}}{\mathrm{d}t}\left(\frac{\partial K}{\partial \dot{q}_i}\right) - \frac{\partial K}{\partial q_i} + \frac{\partial \Pi}{\partial q_i} = Q_i \,, \quad i = 1, \ldots, n \,, \tag{9}$$

where K and Π denote the kinetic and potential energy of the system, respectively, and Q_i is a nonconservative generalized force corresponding to coordinate q_i. Since the virtual work done by reaction forces associated with holonomic constraints is equal zero, generalized forces account for applied forces only. The generalized force that derives from a set of applied forces $\boldsymbol{F}_k$ whose points of application are specified by $\boldsymbol{r}_k$ is defined as

$$Q_i = \sum_k \boldsymbol{F}_k^\mathsf{T} \frac{\partial \boldsymbol{r}_k}{\partial q_i} \,. \tag{10}$$

In case of the wheeled inverted pendulum shown in Figure 1, the horizontal position of the wheel's center of mass, x, and the inclination angle of the rod, φ, are chosen as the generalized coordinates. Defining the zero level for gravitational potential energy to be the level of the wheel's center of mass, the potential energy of the overall system is given by

$$\Pi = m_\mathrm{r} g\ell\cos\varphi \,. \tag{11}$$

With the time derivative of (1) and the rolling constraint (2), the kinetic energy of the system may be expressed as

$$K = \frac{1}{2}\left(m_\mathrm{r} + m_\mathrm{w} + \frac{\Theta_\mathrm{w}}{r^2}\right)\dot{x}^2 - m_\mathrm{r}\ell\dot{x}\dot{\varphi}\cos\varphi + \\ + \frac{1}{2}\left(m_\mathrm{r}\ell^2 + \Theta_\mathrm{r}\right)\dot{\varphi}^2 \,. \tag{12}$$

The motor torque that drives the wheel can be associated with a force couple. As the considered system consists of rigid bodies, the corresponding force vectors are free, that is, their rotational effect is independent of their points of application. Thus, a force couple as shown in Figure 3 may be introduced to exemplify the modeling of the motor torque. The corresponding force and position vectors are given by

$$\begin{aligned} \boldsymbol{F}_1 &= \frac{T}{2r}\begin{bmatrix} -\sin\psi \\ \cos\psi \end{bmatrix} \,, \quad \boldsymbol{r}_1 = \begin{bmatrix} x + r\cos\psi \\ r\sin\psi \end{bmatrix} \,, \\ \boldsymbol{F}_2 &= \frac{T}{2r}\begin{bmatrix} \sin\psi \\ -\cos\psi \end{bmatrix} \,, \quad \boldsymbol{r}_2 = \begin{bmatrix} x - r\cos\psi \\ -r\sin\psi \end{bmatrix} \,. \end{aligned} \tag{13}$$

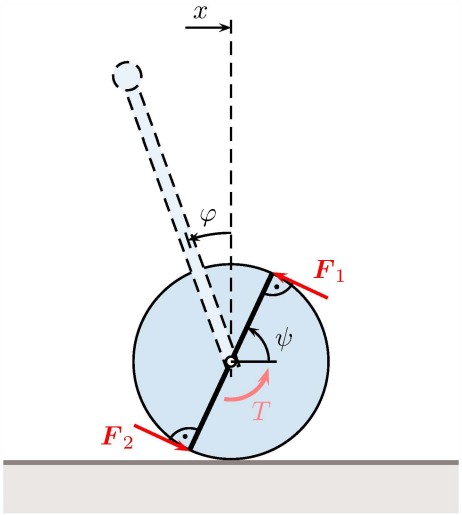

Fig. 3. Force couple associated with the motor torque

Substituting these vectors into (10), it is straightforward to compute the generalized forces of the model as

$$Q_x = -\frac{T}{r} \quad \text{and} \quad Q_\varphi = 0\,. \tag{14}$$

Finally, using (11), (12), and (14), the Lagrange equation (9) yields the governing equations of motion of the wheeled inverted pendulum. Of course, the resulting equations are identical to the previously derived ones stated in (7) and (8), respectively.

III. Simulation

The benchmark model (4) is now compared against the model developed in Section II by means of numerical simulation. Introducing the state variables $z_1 = \varphi$, $z_2 = x$, $z_3 = \dot{\varphi}$ and $z_4 = \dot{x}$, the two models may be expressed in state-space form as

$$\begin{bmatrix} \dot{z}_1 \\ \dot{z}_2 \\ \dot{z}_3 \\ \dot{z}_4 \end{bmatrix} = \begin{bmatrix} z_3 \\ z_4 \\ \boldsymbol{M}(z_1)^{-1} \left(\boldsymbol{f}(z_1, z_3) - \begin{bmatrix} b \\ 1 \end{bmatrix} T \right) \end{bmatrix}, \tag{15}$$

with $b = 1$ representing the benchmark model and $b = 0$ representing the corrected model. The quantities $\boldsymbol{M}$ and $\boldsymbol{f}$ appearing in (15) are defined as

$$\boldsymbol{M} = \begin{bmatrix} \Theta_\mathsf{r} + m_\mathsf{r}\ell^2 & -m_\mathsf{r}\ell\cos z_1 \\ -m_\mathsf{r}r\ell\cos z_1 & \dfrac{\Theta_\mathsf{w}}{r} + (m_\mathsf{w} + m_\mathsf{r})r \end{bmatrix}$$

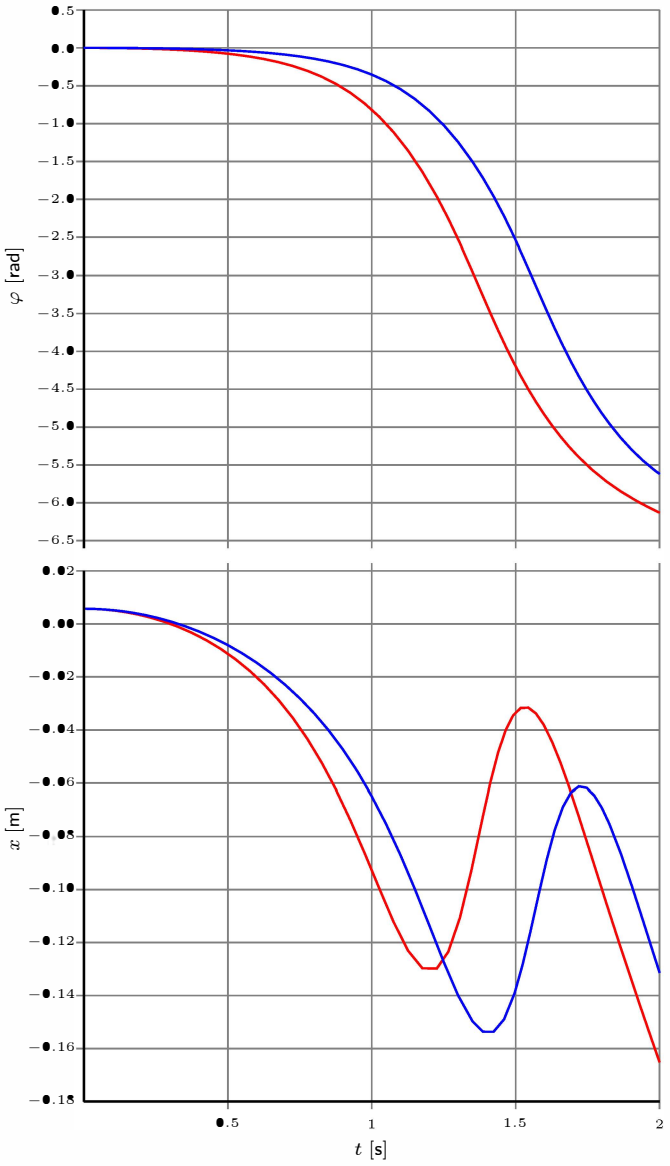

Fig. 4. Step response for $T = 0.1\,\mathsf{Nm}$ (benchmark model, corrected model)

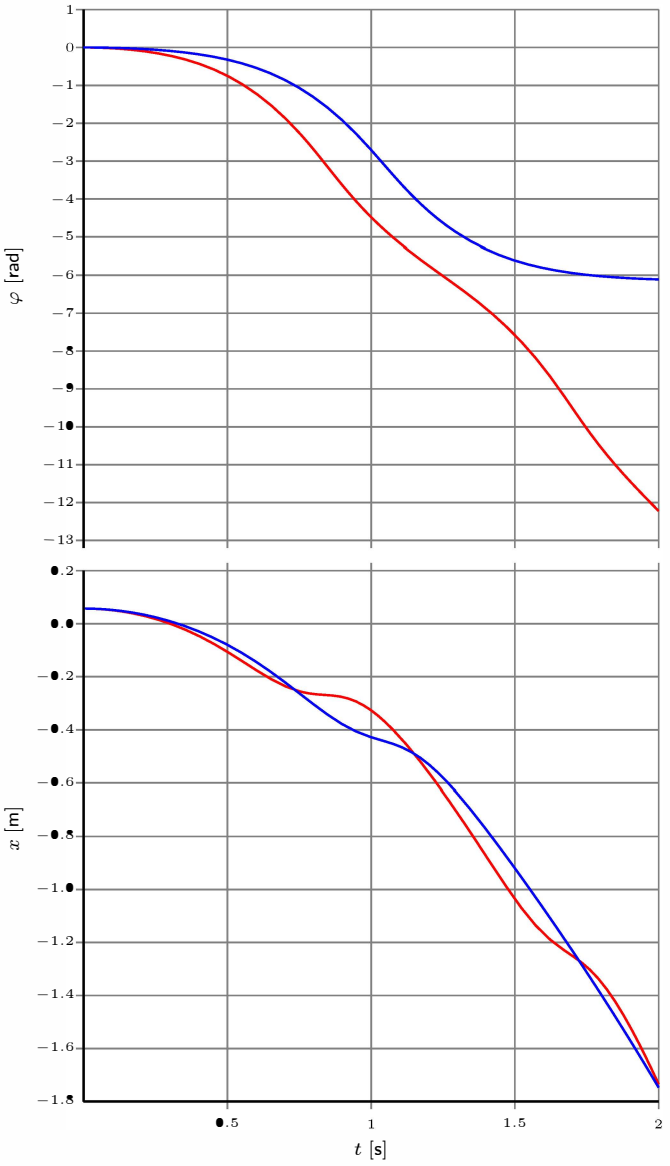

Fig. 5. Step response for $T = 1\,\mathsf{Nm}$ (benchmark model, corrected model)

and

$$\boldsymbol{f} = \begin{bmatrix} g \\ -rz_3^2 \end{bmatrix} m_r \ell \sin z_1 \ ,$$

respectively.

As for the numerical simulation, the initial values of the state variables are all set to zero, while different values are assigned to the motor torque. Figures 4 and 5 show the step responses obtained for $T = 0.1\,\mathrm{Nm}$ and $T = 1\,\mathrm{Nm}$, respectively. While the two models do not differ in case of the unforced system ($T = 0$), the higher the driving torque, the more clearly the deviation appears, at least regarding the inclination angle φ of the rod. As for the horizontal position of the wheel, x, the higher the driving torque, the better the two models agree, because the motion of the rod becomes less effective on the motion of the wheel along with an increasing driving torque.

To decide which of the two models does predict the behavior of the planar wheeled inverted pendulum correctly, one should realize that – as long as no additional effects, such as slippage of the wheel, are considered – the dynamics resembles those of the classical cart-pendulum system. From this, an oscillating motion of the rod is to be expected as indicated in Figure 5 for the model developed in Section II.

IV. Conclusion

The strongly simplified model of a wheeled inverted pendulum is used to illustrate a common misconception in modeling mechanical systems concerning the correct handling of applied and reaction forces and torques, respectively. Of course, many authors refer to the correct model, e. g., Huang et al. [11], but the numerous instances in literature where an erroneous model is used should motivate an in-depth treatment of that issue when teaching applied mechanics.

In a next step, it should be studied how the correction of the model effects the control of such robots.

References

[1] H. G. Nguyen, J. Morrell, et al., Segway Robotic Mobility Platform, SPIE Proc. 5609: Mobile Robots XVII, Philadelphia, PA, October 27-28, 2004.

[2] V. Kurdekar and S. Borkar, Inverted Pendulum Control: A Brief Overview, IJMER, vol. 3, no. 5, pp. 2924-2927, 2013.

[3] Y.-S. Ha and S. Yuta, S., Trajectory tracking control for navigation of the inverse pendulum type self-contained mobile robot, Robotics and Autonomous Systems, 1996.

[4] F. Grasser, A. D'Arrigo, and S. Colombi, JOE: A Mobile, Inverted Pendulum, IEEE Transactions on industrial electronics, vol. 49, no. 1, 2002.

[5] M. Canale and S. Casale Brunet, A Lego Mindstorms NXT Experiment for Model Predictive Control Education, European Control Conference (ECC), Zurich, Switzerland, July 17-19, 2013.

[6] R. C. Ooi, Balancing a two-wheeled autonomous robot, thesis, University of Western Australia, Australia, 2003.

[7] C. Fuhrmann and A. Tenge, Konstruktion und Regelung eines autonomen Zweirad- Roboters, Diploma thesis, University Bielefeld, Germany, 2005.

[8] B. Carlsson and P. Örbäck, Mobile inverted pendulum – control of an unstable process using open source real-time operating system, Master thesis, Chalmers University of Technology, Gothenburg, Sweden, 2009.

[9] B. Bonafilia, N. Gustafsson, and S. Nilsson, Self-balancing two-wheeled robot, report, Chalmers University of Technology, Gothenburg, Sweden, 2013.

[10] S. W. Nawawi, M. N. Ahmad, and J. H. S. Osman, Real-Time Control of a Two-Wheeled Inverted Pendulum Mobile Robot, World Academy of Science, Engineering and Technology, vol. 2, no. 3, 2008.

[11] J. Huang, Z.-H. Guan, et al., Sliding-Mode Velocity Control of Mobile-Wheeled Inverted-Pendulum Systems. IEEE Trans. Robotics, volume 26(4), pages 750758, 2010.